

Some New Observations on Freckle Formation in Directionally Solidified Superalloy Components

DEXIN MA, QIANG WU, and ANDREAS BÜHRIG-POLACZEK

To improve the understanding of freckle formation in superalloys, several directional solidification experiments were carried out in a production-scale Bridgman furnace. During the careful inspections of the many cast specimens, several interesting phenomena were observed, indicating new aspects of freckle formation. Accordingly, several new factors influencing the freckle formation, such as the shadow effect, the edge effect, the step effect, and the crystal orientation effect, are proposed. This will contribute to our current understanding of freckle formation and the future development of new measures to minimize freckle defects in directionally solidified components of superalloys.

DOI: 10.1007/s11663-011-9608-0

© The Minerals, Metals & Materials Society and ASM International 2011

I. INTRODUCTION

FRECKLES have attracted the attention of researchers for more than 40 years since the pioneering works by Giamei *et al.*^[1,2] Freckles are a detrimental grain defect observed in directional solidification (DS) and single-crystal (SC) castings of superalloys leading to a high rejection rate. They appear as long trails of equiaxed (EQ) grains, aligning roughly parallel to the direction of gravity. It is commonly believed that freckles are formed as a result of the thermosolutal convection induced by inverse density in the mushy zone.^[2] During upward directional solidification, the interdendritic melt can become gravitationally unstable because of the chemical segregation of alloying elements. The density difference between the less dense solute in the mushy zone and the bulk liquid ahead of the dendrite tip can cause thermosolutal convection when the driving force for the fluid flow exceeds the surrounding frictional forces. Because of the remelting and fragmenting of the dendrite arms, freckles may appear. Once a freckle chain has formed in a fully solidified crystal, it is impossible to remove such an undesired defect through thermal treatments.

Generally, the occurrence of freckles is known to be dependent mainly on three factors: alloy chemistry, solidification parameters, and casting size.^[1,3] First, the probability of freckle occurrence has been found to be strongly dependent on the composition of the alloys.^[1,2,4,5] As the level of refractory alloying additions to SC superalloys has increased to improve high-temperature mechanical properties, freckle formation during DS has increasingly become a serious problem. Although freckles can be reduced potentially by optimizing the levels of Ta, W, and Re, this is unlikely to

benefit phase stability, corrosion, and creep fatigue properties simultaneously. Therefore, alloying alternatives that improve solidification characteristics without significantly compromising the physical and mechanical properties of the alloys are highly desirable.^[4] Another factor playing an important part in freckle formation is the solidification condition. The process parameters affect directly the dendrite spacing and the permeability of the mushy zone. A lower temperature gradient G and solidification velocity V result in the larger dendrite spacing and higher permeability. This result promotes convective flows in the mushy zone and assists the formation of freckles. Finally, the extent of freckling becomes more pronounced as the casting size increases.^[1,4,6,7] When a casting is of significant cross-sectional area, the wide mushy zone can provide a sufficient reservoir to support the interdendritic convection and, hence, the freckling onset. Therefore, for a defined alloy system and casting process, the components with a larger cross section are more freckle prone. In contrast, freckles are normally not present in components of small size.^[1]

The recent studies pertaining to freckle formation have concentrated on the development of computational process models^[8–17] and the incorporation of Rayleigh-based criteria to describe the onset of thermosolutal convection and subsequent formation of grain defects.^[18–26] However, these models and criteria cannot be applied simply to predict the freckle formation in the industrial production because the solidification condition and the dendrite growth in the component cluster are complicated. To meet the requirements of material property and mechanical function, the superalloy composition and casting geometries are designed specially and cannot be changed arbitrarily to prevent the freckle formation. The common industrial solution to minimize the freckle formation in DS castings, *i.e.*, increasing the temperature gradient to decrease the dendrite spacing, has clear limitations because of many factors such as the poor thermal conductivity of the shell molds. As the size

DEXIN MA, Senior Scientist, QIANG WU, Ph.D. Student, and ANDREAS BÜHRIG-POLACZEK, Professor, are with the Foundry Institute, RWTH University, Aachen 52072, Germany. Contact e-mail: d.ma@gi.rwth-aachen.de

Manuscript submitted May 5, 2011.

Article published online November 29, 2011.

of the superalloy castings becomes larger, it is increasingly difficult to maintain a high thermal gradient in a conventional Bridgman furnace. Therefore, more efforts should be made to detect all possible factors influencing freckle formation during the casting process and to find additional technical measures to reduce the undesired grain defect.

II. EXPERIMENTAL

Because of its increasing importance, the phenomenon of freckle formation in superalloys has in recent years also become the subject of intensive research efforts at the Foundry Institute of RWTH Aachen University. To understand freckling under industrial conditions, several directional solidification experiments were carried out in a production-scale vacuum Bridgman furnace. The superalloy used is CMSX-4 (Cr 6.5, Co 9.0, Mo 0.6, W 6.0, Al 5.6, Ta 6.5, Ti 1.0, Re 3.0, and Hf 0.1 in wt pct) because it is a typical freckle-prone superalloy.^[27] As most single-crystal, Ni-base superalloys exhibit an inherent tendency to form convective instabilities during directional solidification,^[6] the results gained are generic for conventional superalloys, especially for those prone to freckle formation.

Different component geometries, for example, cylindrical bars with constant or varied diameter, were used to identify their influence on the freckle formation. In each shell mold cluster, the components were assembled around a central rod. The shell molds were produced by a standard investment casting procedure. The selector method was used for the single-crystal solidification of the components. To measure the temperature development in the components, thermocouples were placed at defined positions. For each casting experiment, a ceramic shell mold was placed on the copper chill plate in the Bridgman furnace. The shell mold cluster was preheated, poured with superalloy melt, and then withdrawn out of the heating zone through the baffle into the cooling zone. In these experiments, a heater and pouring temperature of 1773 K (1500 °C) was used. A low withdrawal velocity of $V = 1$ mm/min was applied to promote the freckle formation.

After the casting experiment, the shell mold was cooled down in the furnace. When the temperature in the furnace reached approximately 473 K (200 °C), the vacuum was released and the entire casting mold was removed. The cast part was then knocked out of the ceramic mold and the components were separated appropriately from the casting cluster. Finally, the casting was sand blasted to remove any ceramic attached to its surface. Macroetching and metallographic examination were employed to determine the freckle defect in the directionally solidified specimens. No chemical analyses were performed for the segregation of alloying elements.

During the careful inspections of a large number of cast specimens, several interesting phenomena about freckle formation were observed. Correspondingly, some new factors influencing freckle formation were detected.

III. RESULTS AND NEW OBSERVATIONS

A. Shadow Effect

For the DS process, the components were arranged in a circle around a central rod (Figures 1(a) and (b)). In all performed experiments, the freckles were found exclusively on the “shadow side” of the samples (Figures 1(b) and (d)), which faces the central rod and could not be irradiated directly by the heater. On the other side facing the heater, no freckles were observed. This shadow effect indicates an unsymmetrical thermal condition between the inner and outer side of the casting cluster and exhibits an important influence on freckling.

From the measured cooling curves (Figure 1(c)), the temperature gradient on the shadow and heater side was determined to be 2.3 K/mm and 2.8 K/mm, respectively. This difference in temperature gradient is relatively small and should not be the decisive factor for the freckle onset exclusively on the shadow side of all specimens. In fact, the metallographic examination of the specimen sections shows no remarkable difference in the dendrite spacing between the shadow and the heater side. The reason for the unsymmetrical distribution of the freckle defect must be the different curvature of the solidification front. As shown schematically in Figure 1(a), the shadow and heater side of a specimen have a concave and a convex isotherm, respectively, revealing a significantly different freckling condition. Auburtin and co-workers^[3,28–30] have suggested that freckle formation is strongly related to the shape of the macroscopic interface associated with isotherms. The observation in this work also confirmed the promoting effect of the concave isotherm on the freckle formation.

In previous works of the authors,^[31,32] the shadow effect has been identified to be a promoting factor for the stray grain defect. The current work shows the shadow effect on the freckle formation for the first time. It should be noted that this effect occurs only in the components solidified in cluster, where the shadow side facing the central rod was heated ineffectively because of the radiation hindrance in the radical alignment. In the laboratory-scale investigation, the single samples are normally produced individually by a vertical directional solidification process. Because of the absence of the shadow effect, the freckles were hardly observed, although the process condition was controlled to be particularly favorable for freckle formation.^[3,28,29,33] This gives a full confirmation of the shadow effect on the freckling from another side. It can then be expected that the freckle defect in the real components of superalloys will be reduced significantly if they are cast individually instead of in cluster. This is especially important for the production of the components requiring high quality where no freckles are tolerated, even though the productivity of the castings has to be reduced significantly.

B. Edge Effect

As shown in Figure 1, two samples (numbers 3 and 4) in the cluster have a rectangular cross section. Because of the shadow effect, the freckles are observed only on both edges in the shadow sides of each specimen, whereas no freckles could be found on the planes facing

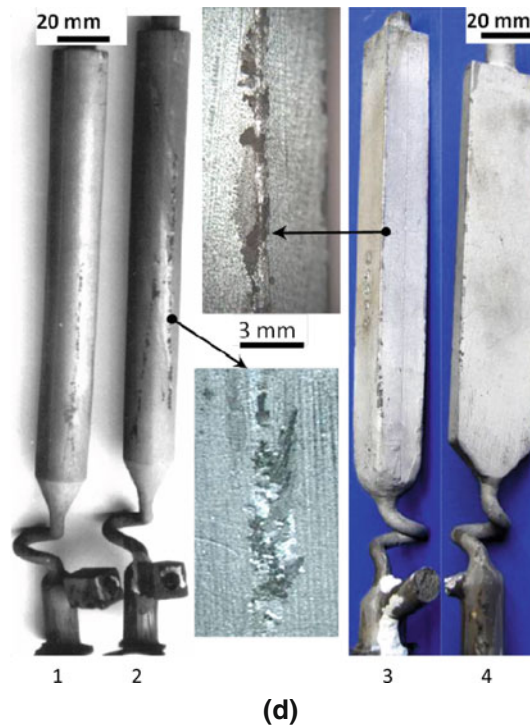
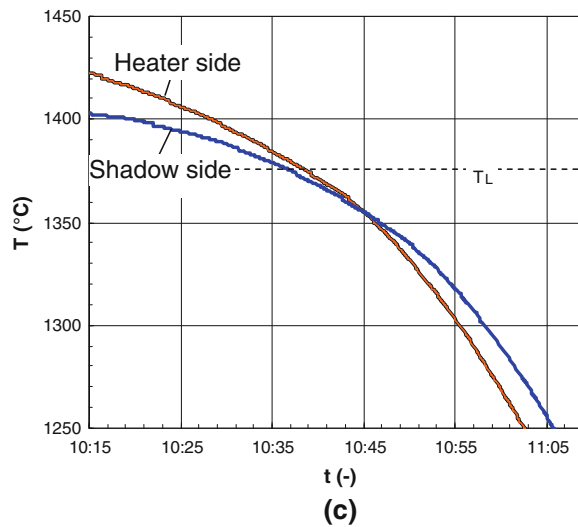
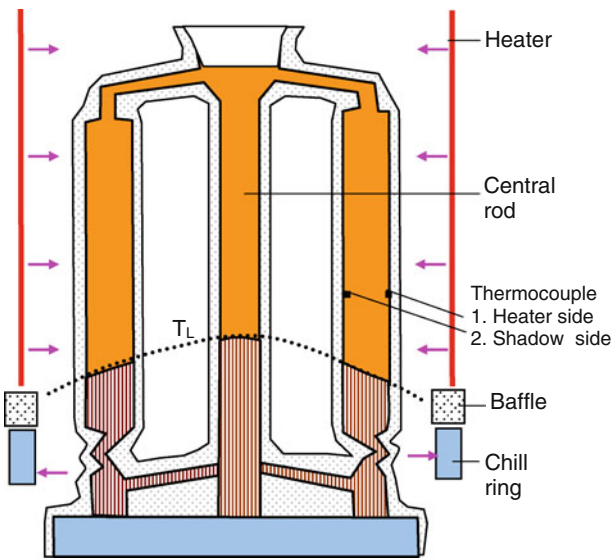


Fig. 1—Schematic representation of the component arrangement in the Bridgman furnace: (a) longitudinal section, (b) cross section, and the measured cooling curves on the shadow and heater side of a specimen (c). (d) The freckle chains on the shadow side of the cylindrical (numbers 1 and 2) and rectangular-shaped samples (numbered 3 and 4) solidified in a cluster.

the central rod directly. This phenomenon cannot be explained with the current scientific knowledge. Ordinarily, the edges of the samples have the best cooling condition and can solidify faster than anywhere else, resulting in a better thermal condition to suppress the freckle formation. Therefore, it is normally believed that freckles arise preferentially on the smooth surfaces of the superalloy components. However, the observation in Figure 1 indicates clearly the promoting effect of the edge geometry on the freckle formation. The reason may be the concave isotherm and the better permeability along the edge of the shell mold cavity.

In the platform of a large dummy turbine blade cast in a previous experiment with the same alloy CMSX-4, the freckle formation on the edges was found also to be more pronounced than that on the plane surface (Figure 2). This observation confirms once again the edge effect promoting freckle formation.

C. Step Effect

In the cylindrical specimens with abruptly varying cross sections, which were cast in cluster, the freckles also were found also only on the shadow sides of the specimens.

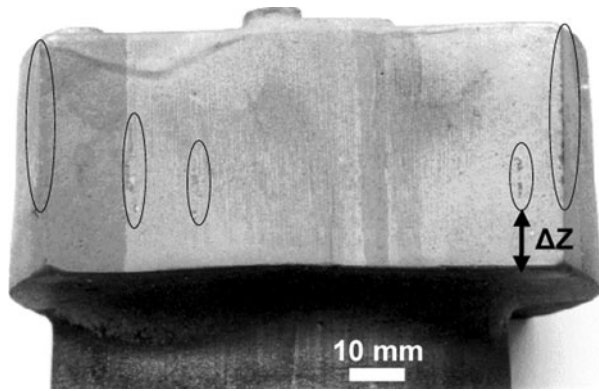


Fig. 2—Freckle formation (indicated with ellipses) in the platform of a large dummy turbine blade.

In the sample shown in Figure 3(a), the diameter was increased stepwise from 10 mm to 15, 20, and 25 mm. After each expansion, the freckle chains were not formed immediately but at an incubation distance of approximately $\Delta Z = 10$ mm above the bottom edge of the steps (Figures 3(a1) to (a3)). This step effect can also be observed in the turbine blade shown in Figure 2, where the freckles chains start at approximately $\Delta Z = 10$ mm above the platform bottom. It is postulated that the freckle channel must draw liquid from a reservoir in the solidifying network with a minimum volume.^[10] Freckles should not develop in casting areas where this condition is not met. Therefore, the incubation distance found in Figures 2 and 3 must be a minimum length of the mushy zone to stimulate the interdendritic convection for the formation of freckles. It can be reasonably expected that the freckle formation can be avoided if the step length after a dimension expansion is limited to be shorter than the incubation distance.

In the sample shown in Figure 3(b1), the diameter was first expanded to 25 mm and then decreased to 20 and 15 mm. In the bottom section of the sample, the freckle chain B was formed with an incubation distance caused by the same expanding effect as shown in Figure 3(a). With the following decrease in sample dimension in the direction of solidification, however, the freckle chains C and D could arise immediately at the bottom of the steps without any incubation (Figures 3(b1) to (b3)). That means the incubation distance ΔZ becomes 0. It is interesting to point out that the onset of the freckle chains C and D were attributed clearly to the abrupt dimension contraction. After that, the freckles could not grow too far along the smooth surfaces.

Figure 4 gives two more examples for the step effect of contracting dimension on the freckle onset. In these specimens with varying cross section, the freckles are not observed in the larger diameter section, but in the significantly thinner ones. The freckles arise just after the decrease in cross section. At a distance of approximately 10 mm after the section transition, the specimens become freckle free again because it is beyond the promoting effect of the contracting dimension on the freckle onset.

According to the well-known size effect, the specimens should become less freckle prone as the diameter

decreases. In Figures 3(b) and 4, however, the opposite phenomenon was observed. Additionally, when a solid/liquid interface goes through the decreased cross section, the local heat extraction would be enhanced, and there is an increase in the local cooling rate and in the vertical thermal gradient. This indicates an unfavorable thermal condition for freckle formation. The observed freckle onset just at this location is then also inconsistent with the well-known effect of solidification parameters on the freckle formation. The reasonable explanation would probably be the wide mushy zone under the contracting section providing sufficient interdendritic convective flow to support the freckle formation.

The step effect of expanding dimension on the freckle formation is analyzed schematically in Figure 5. As stated, freckles in directionally solidified superalloys occur preferentially on the external surface of the castings because of the significantly better permeability along the mold/casting interface. At the abrupt expansion of the sample, the old freckle chain on the surface of the lower section cannot grow any more because of the ending of the vertical surface. Although a new vertical surface is available after an abrupt expansion of the cross section, the freckles cannot arise immediately at the bottom edge of the new surface. The thermosolutal convection current resulting in freckling can occur only when a sufficient supporting volume in the new section is established (Figure 5(a)). It is just in this supporting zone that the alloying segregation and density inversion will be built up sufficiently, providing the driving force strong enough to initiate the convection current for freckling along the mold/casting interface. Therefore, the incubation height ΔZ shown in Figures 2 and 3(a) must be the minimum length of the new supporting zone for the formation of the new freckles.

At the abrupt contraction of the sample (Figure 5(b)), the freckle chains can arise immediately on the new surface as a result of the available mushy zone below the bottom edge of the new surface. Because of the larger dimension of the lower section, significantly more reservoir volume is provided to stimulate the thermosolutal convection for freckle formation than in the samples without geometry variation. During subsequent solidification the mushy zone in the lower section is exhausted, and the promoting effect of the contracting dimension on the freckling disappears. As a result, no new freckles are formed at a distance after the section transition (Figure 4).

Because of the observed step effect on the freckle formation, a corresponding method to prevent freckle defects can be proposed. The components with varying cross section should be solidified in the direction of the increasing dimension instead of the decreasing dimension. As mentioned previously, the freckle formation can be avoided if the step length after a dimension expansion is shorter than an incubation distance of approximately 10 mm.

D. Crystal Orientation Effect

As mentioned in the previous section, specimens with a larger diameter do not necessarily mean more freckle

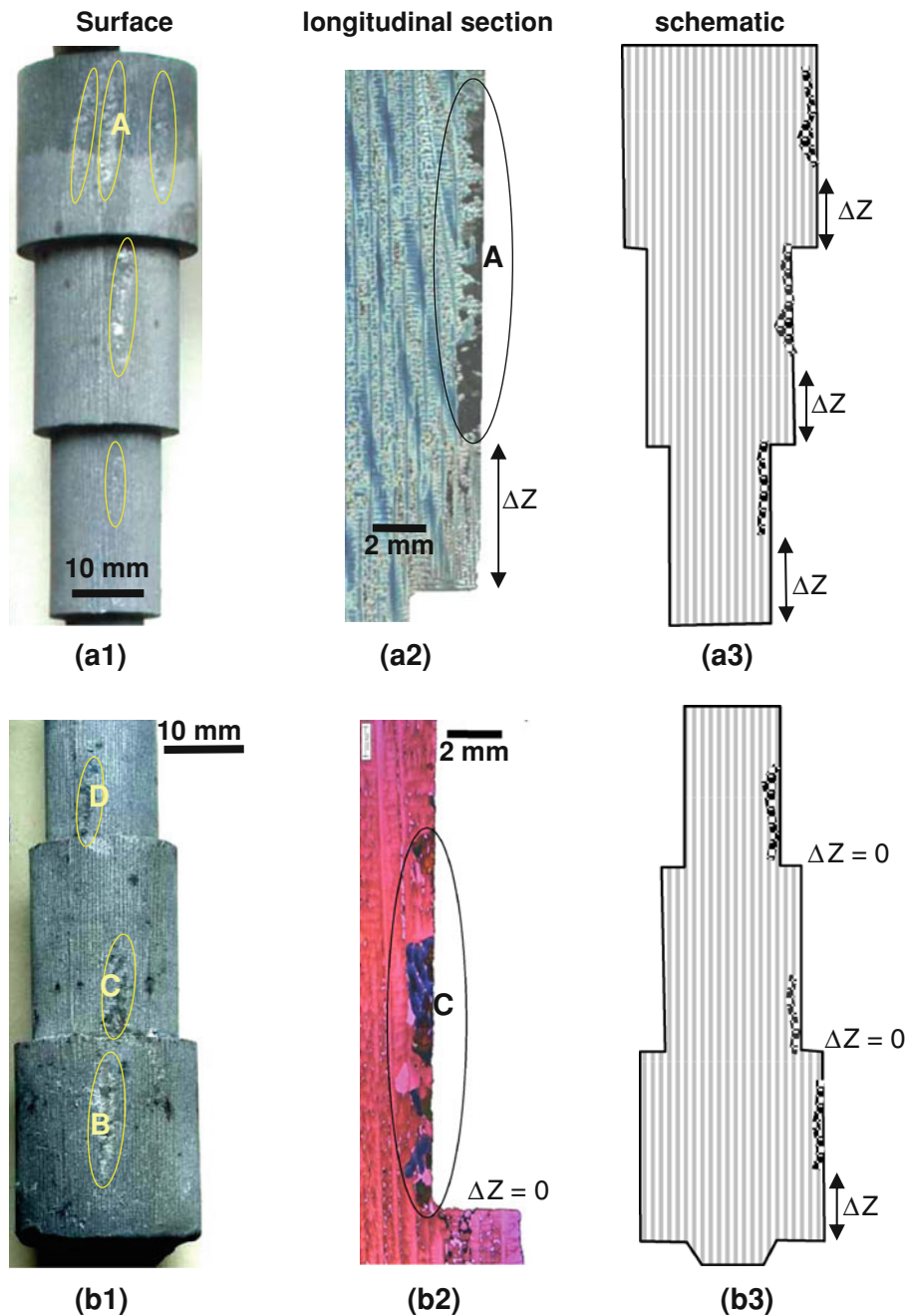


Fig. 3—Freckle formation in the samples with stepwise increasing (a) and decreasing diameter (b). The length ΔZ indicates the incubation distance for the freckle onset after varying the specimen diameter.

formation. Several more examples can be found in Figure 6. The freckles appeared in the slenderer specimens (A and B), while the much thicker samples (C and D) remained freckle free. By inspecting the etched surface carefully, it can be found that in the specimens with freckles, the dendrites are aligned roughly parallel to the long axis of the specimens, whereas in the specimens without freckles, the dendrite alignment is inclined clearly. Because the alignment of the dendrites is defined by the crystal orientation, it seems that the freckle formation is influenced strongly by the crystal orientation of the specimens.

To examine this correlation, the crystal orientation of the samples was measured by electron backscatter diffraction and shown in the pole figures in Figure 6. In the specimens with well-aligned dendrites, as expected, the [001]-orientation is nearly identical to the specimen axis and, hence, to the solidification direction. In this case, the specimens are prone to freckle formation despite their small diameter (specimen A and B). In contrast, in the specimens with poorly aligned dendrites, no freckles have been observed, although their diameter is significantly larger (specimen C and D).

It should be pointed out that all single crystal specimens shown in Figure 6 were solidified vertically in the same shell mold cluster and, hence, under the same process condition. The only difference besides their diameter is their crystal orientation with respect to gravity. Therefore, it is proven that the freckle formation is noticeably more sensitive to the dendrite orientation than to the component diameter. Obviously, the vertically aligned dendrite arrays have the best interdendritic permeability for the upward convection in the mushy zone. The inclination of the dendrite arrays could lead to an increase in their flow resistance. As a result, the interdendritic liquid should be stabilized, leading to the suppression of the formation of freckle defects.

To investigate the flow behavior in the dendritic mushy zone, a computer simulation was performed by using the form-filling module of the comprehensive

simulation software MAGMASOFT (MAGMA Gießereitechnologie GmbH, Aachen, Germany).^[34] The mushy zone was represented by the core in this module, which shall remain solid during the form filling, and it has the same geometry as the dendrite networks. These dendrites were placed in different orientations in the casting cavity. As reference, the columnar dendrite array was first aligned vertically to exhibit the [100] orientation of the dendrites in the long axis of the casting antiparallel to the gravity direction (Figure 7(a)). The other orientations can be realized also by inclining the dendrite arrays in defined directions to defined degrees (Figure 7(b) through (f)). After the entrance of the melt into the casting cavity, a stable flow can soon be established. Figure 7 shows the simulated melt flow state within the investigated dendrite networks at the same filling time (10 seconds after pouring), which reveals the relationship between the height of the melt flow front and the dendrite orientations. As can be observed, the upward flow front in the dendrite array with a [100] orientation advanced the most (Figure 7(a)). With increase in dendrite inclination, the melt flow slows down continually. It is then reasonable to assume that the melt flows more easily along the channels among the primary dendrite trunks than in any other direction. For the vertical dendrite array, the driving force and the primary dendrite trunks are identical, thus enabling the fast melt flow. When the dendrites are inclined to a defined angle, the vertical melt flow must pass through the dendrite trunks with the same angle. By increasing the inclination angle, more dendrite trunks have to be passed through, which leads to the increase in the resistance to the upward flow. As is well known, freckles are believed to be generated as a result of thermosolutal convection in an upward direction against the dendrite resistance. Thus, the well-orientated single crystal castings are more freckle prone because the vertical aligned dendrite arrays have the best permeability and are,

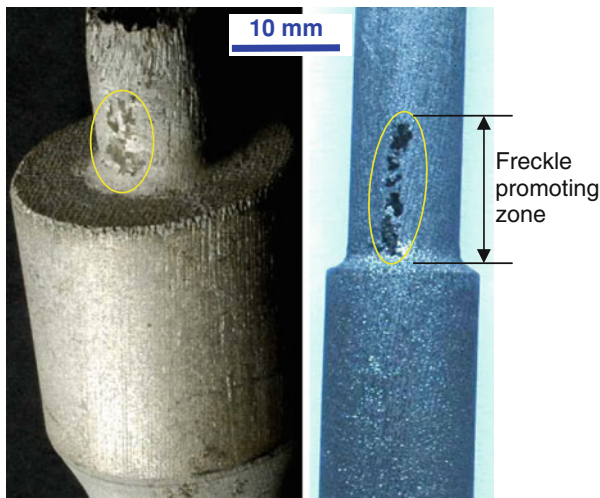


Fig. 4—Examples showing freckle formation after a contraction of the cross section despite the significant decrease in diameter.

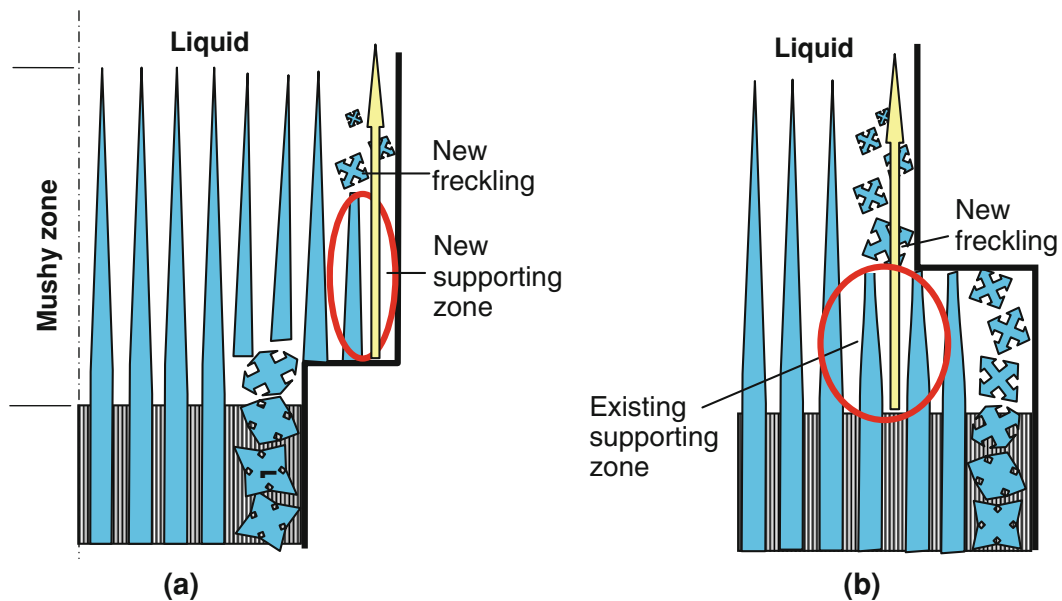


Fig. 5—Schematics of freckle development at an abrupt enlargement (a) and at a contraction of the cross section (b).

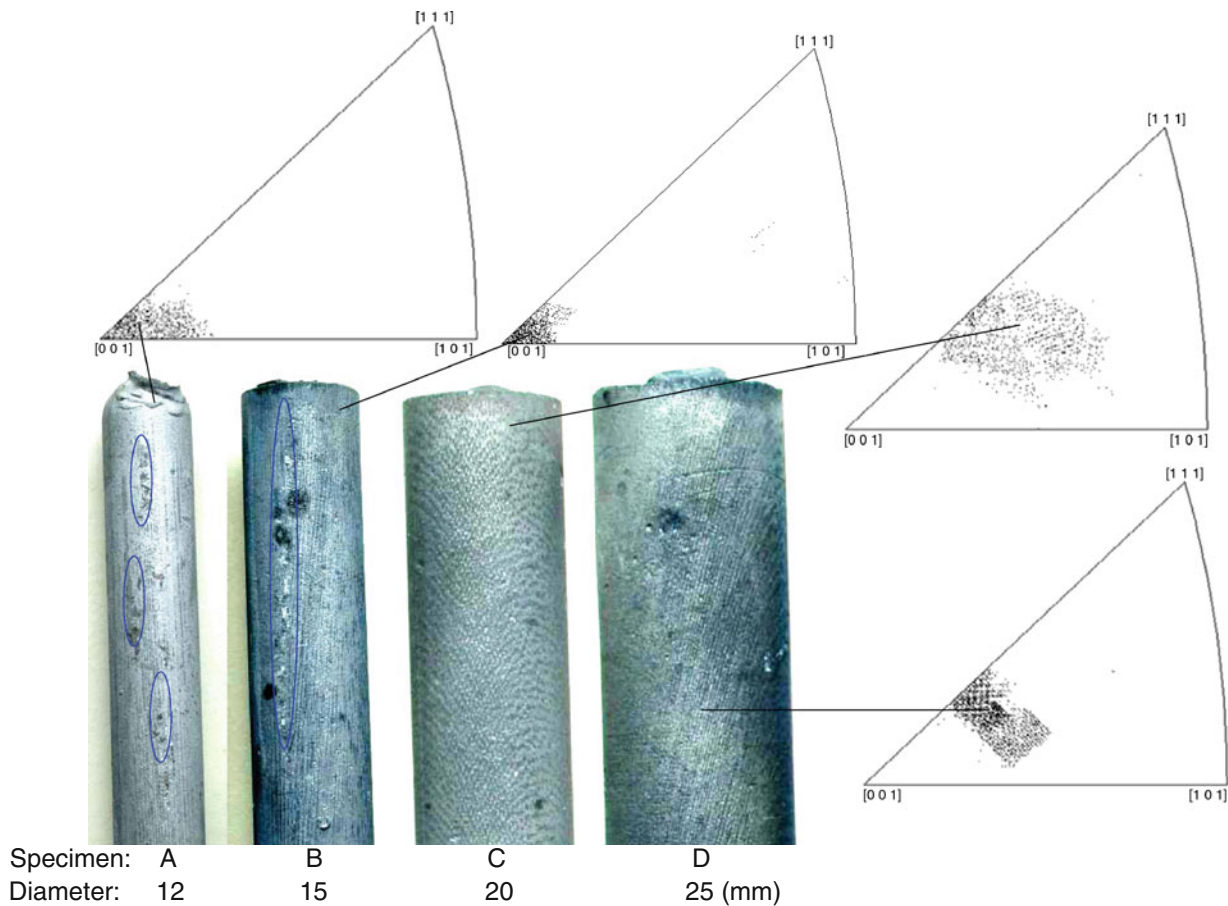


Fig. 6—Photographs of the SC specimens with different diameters and pole figures exhibiting their crystal orientations. The ellipses indicate the freckles, which occur only in the well aligned specimens (A and B), despite their smaller diameters.

therefore, favorable for the onset of the vertical thermosolutal convection. In contrast, the inclination of the dendrites becomes a stabilizing factor for the interdendritic liquid to suppress the vertical thermosolutal convection and the subsequent formation of freckle defects.

Auburtin *et al.*^[29] studied the influence of the solidification front angle on freckle formation by tilting the Bridgman-furnace used for DS experiments. It was found that tilted castings exhibited freckles, whereas vertical castings were freckle free. In the current work, however, all SC specimens with different crystal orientations were solidified vertically without any tilting. As a result, the influence of crystal orientation on the freckle formation was detected. This could add new insight toward understanding the freckle arising mechanisms. Furthermore, the dependence of freckling on crystal orientation should be taken into account in the modeling and simulation to provide a more accurate prediction of freckle formation in superalloy castings.

E. Internal Freckle Formation

Internal freckles were often observed in directionally solidified samples of transparent model systems and Pb alloys.^[2,23,35–37] For superalloys, internal freckles could

be detected only in vacuum-arc remelting and electroslag remelting processed ingots.^[28,38] They are located mostly in a region between the center and the midradius of the as-cast ingot. Freckles in the midradius have distinct streak profiles, whereas those in the center region have an irregular shape.^[38] In the directional solidification of superalloys, however, virtually all freckles found occur at the external surface of the castings (mold/casting interface), whereas none have been found inside the castings.^[1,2,4] But in our experiments, as shown in Figure 8, internal freckles were also observed in a directionally solidified cylindrical specimen at a diameter increase from 10 to 15 mm. The freckle chain consisting of equiaxed grains is located just in the middle of the specimen. In the longitudinal sections, it looks the same as those formed at the specimen surface. This is probably because of the disturbance of the equilibrium state at the interface and the perturbation in the dendrite growth resulting from the abrupt variation of the cross section.

The occurrence of freckles inside of the superalloy components might be a large problem because they cannot be detected without the castings being cut open, even by ultrasound. Fortunately, this kind of internal freckles is only an accidental phenomenon. In fact, during the inspection of nearly 100 specimen sections in

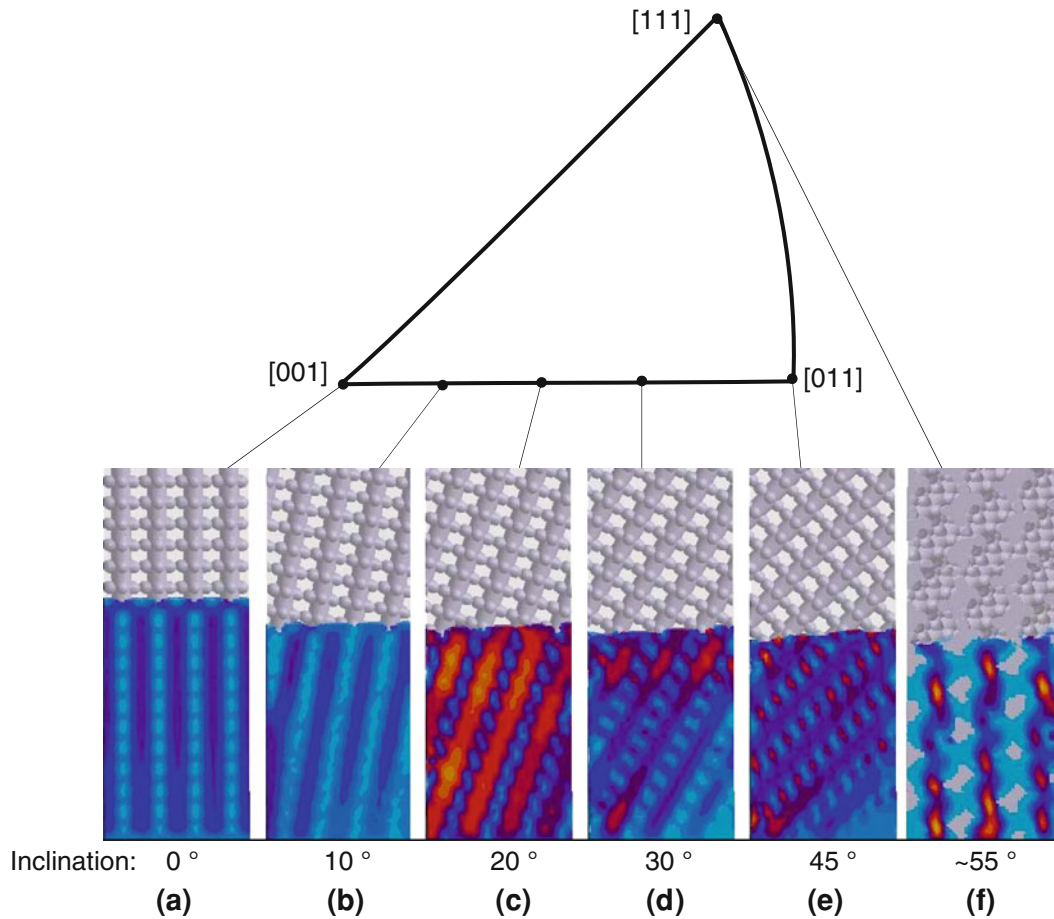


Fig. 7—Simulated flow front position in the mushy zone with different dendrite inclinations at the same filling time. In the [001] orientation, the fastest flow is predicted; with an increase in the dendrite inclination, the flow slows down continually.

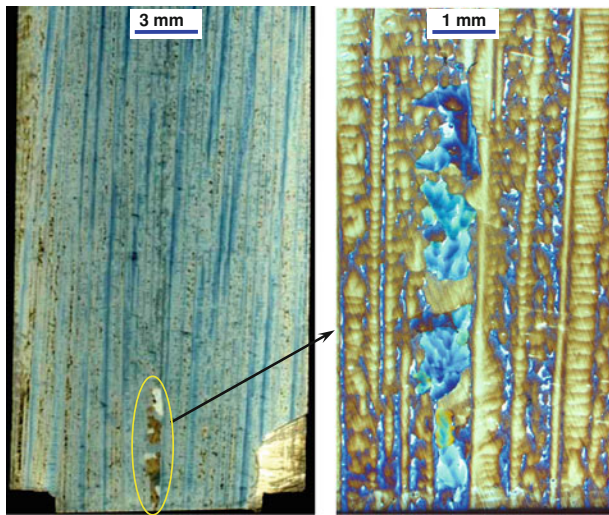


Fig. 8—Longitudinal sections showing a freckle chain in the middle of a specimen.

our research work, only one internal freckle chain was found as shown in Figure 8. However, to insure an absolutely high operational reliability of the superalloy components under high temperature, it is necessary to develop a method to inspect such internal grain defects.

F. Freckles in Equiaxed Grains

It is believed that freckles are a typical grain defect in superalloy components solidified directionally with a columnar structure. However, in an additional experiment, when we used a low heater temperature of 1723 K (1450 °C), freckles were found in the specimens with an EQ grain structure (Figure 9). Because of the low temperature gradient of approximately 1.2 K/mm, the nucleation of new grains ahead of the solid/liquid interface becomes energetically feasible. The grains nucleate at the mold wall and grow into the undercooled melt with a random crystallographic orientation, resulting in a solidification structure consisting solely of EQ grains. It is interesting to note that the freckle chains could still grow upward through different equiaxed grains, although no directional growth of columnar dendrite arrays was available.

As indicated in Section III-E, no freckles have been detected in the SC specimens when the dendrites were inclined clearly. In Figure 9, it can be found that the dendrites orientation in most EQ grains deviates far from the specimen axis. For this reason, it is difficult to distinguish the primary and secondary dendrites in these EQ grains. That means the freckle formation in the specimens with inclined dendrites can take place, but only under an extremely poor thermal condition so that

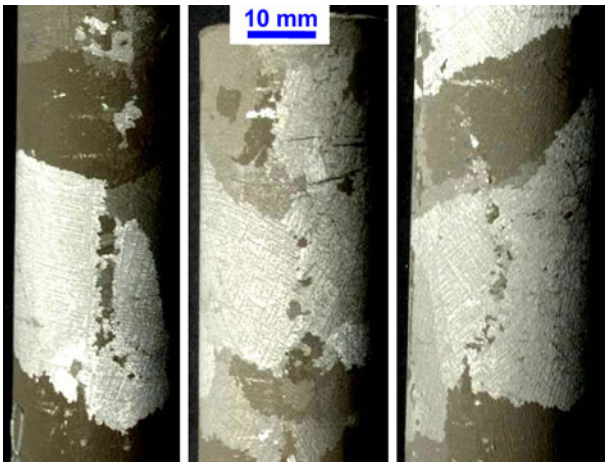


Fig. 9—Freckles observed in equiaxed grain structure of the superalloy specimens.

no directional and single-crystal growth is possible. The freckle formation in the EQ structure should be investigated to better understand the mechanisms of the freckle formation.

IV. SUMMARY

In the current work, several directional solidification experiments were carried out under industrial conditions. By an inspection of cast specimens, some interesting phenomena about freckle formation were observed. This will contribute to a better understanding of freckle formation in directionally solidified components of superalloys. Correspondingly, some new measures are proposed to minimize the freckle defect.

In all specimens cast in cluster, freckles were found exclusively on the “shadow side” of the samples facing the central rod, whereas no freckles formed on the side facing the heater. It can then be expected that the freckle defect in the real components of superalloys will be reduced significantly if they are cast individually instead of in cluster.

In the specimens with rectangular-shaped cross section, the freckles were observed on the edges instead of on the plane surface, although the cooling condition on the edges was unfavorable for the freckle formation.

In the specimens with stepwise increasing cross sections, the freckle chains were not formed immediately at the bottom edge of the steps, but after an incubation distance of about 10 mm, indicating a suppressing effect on the freckling. In contrast, contracting the dimension reveals a promoting effect on the freckle onset. Considering the step effect, it is proposed to solidify the components in the direction of increasing dimension to avoid the freckle defect effectively.

Freckle formation is influenced strongly by the crystal orientation of the specimens. Aside from the conventional knowledge that freckles are promoted by larger casting size, the specimens with a good [001] axial orientation exhibited freckles despite their small diameter. In contrast, the bigger diameter samples can remain

freckle free because of the deviation of the primary dendrites from the solidification direction.

Freckle formation was also found inside a DS specimen and in the EQ structure. This is also inconsistent with our common knowledge that freckles occur at the external surface of the DS superalloy castings with columnar structure.

ACKNOWLEDGMENTS

This work was supported by the Deutsche Forschungsgemeinschaft (DFG) through Grant BU1072/15-1 and -2. Appreciation is extended to S. Hollad, J. Norminikat, D. Lembrecht, and E. Schaberger-Zimmerman for their assistance in the experiments.

REFERENCES

1. A.F. Giamei and B.H. Kear: *Metall. Trans.*, 1970, vol. 1, pp. 2185–92.
2. S.M. Copley, A.F. Giamei, S.M. Johnson, and M.F. Hornbecker: *Metall. Trans.*, 1970, vol. 1, pp. 2193–204.
3. P. Auburtin, S.L. Cockcroft, and A. Mitchell: *Material for Advanced Power Engineering 1998, Proceedings of the 6th Liege Conference*, Part III, J. Lecomte-Beckers, F. Schubert, and P. Ennis, eds., Uni. De Liege European Commission, pp. 1459–68.
4. S. Tin: Ph.D. Dissertation, University of Michigan, Ann Arbor, MI, 2001.
5. R.A. Hobbs, S. Tin, and C.M.F. Rae: *Metall. Mater. Trans. A*, 2005, vol. 36A, pp. 2761–73.
6. S. Tin and T.M. Pollock: *J. Mater. Sci.*, 2004, vol. 39, pp. 7199–205.
7. S. Tin, T.M. Pollock, and W.T. King: *Superalloy 2000*, T.M. Pollock, R.D. Kissinger, and R.R. Bowman, eds., TMS, Warrendale, PA, 2000, pp. 201–10.
8. S.D. Felicelli, J.C. Heinrich, and D.R. Poirier: *Metall. Trans. B*, 1991, vol. 22B, pp. 847–59.
9. M.C. Schneider and C. Beckermann: *Metall. Mater. Trans. A*, 1995, vol. 16A, pp. 2373–88.
10. M.C. Schneider and C. Beckermann: *ISIJ Int.*, 1995, vol. 35, p. 665.
11. S.D. Felicelli, D.R. Poirier, and J.C. Heinrich: *J. Crystal Growth*, 1997, vol. 177, pp. 145–61.
12. M.C. Schneider, J.P. Gu, C. Beckermann, and U.R. Katterner: *Metall. Mater. Trans. B*, 1998, vol. 29B, pp. 847–55.
13. C. Frueh, D.R. Poirier, and S.D. Felicelli: *Mater. Sci. Eng. A*, 2002, vol. 328, pp. 245–55.
14. M. Medina, Y. Du Terrail, F. Durand, and Y. Fautrelle: *Metall. Mater. Trans. B*, 2004, vol. 35B, pp. 743–53.
15. J. Jain, A. Kumar, and P. Dutta: *J. Phys. D: Appl. Phys.*, 2007, vol. 40, pp. 1150–60.
16. R.F. Katz and M.G. Worster: *J. Comp. Phys.*, 2008, vol. 227, pp. 9823–40.
17. L. Yuan and P.D. Lee: *ISIJ Int.*, 2010, vol. 50, pp. 1814–18.
18. S. Chandrasekhar: *Hydrodynamics and Hydromagnetic Stability*, Clarendon Press, Oxford, UK, 1961, pp. 9–10.
19. J.R. Sarazin and A. Hellawell: *Adv. Phase Transit.*, 1987, vol. 10, pp. 101–15.
20. C. Beckermann, J.P. Gu, and W.J. Boettinger: *Metall. Mater. Trans. A*, 2000, vol. 31A, pp. 2545–52.
21. J.C. Ramirez and C. Beckermann: *Metall. Mater. Trans. A*, 2003, vol. 34A pp. 1525–35.
22. S.N. Tewari and R. Tiwari: *Metall. Mater. Trans. A*, 2003, vol. 34A, pp. 2365–76.
23. S.N. Tewari, R. Tiwari, and G. Magadi: *Metall. Mater. Trans. A*, 2004, vol. 35A, pp. 2927–34.
24. Q. Feng, L.J. Carroll, and T.M. Pollock: *Metall. Mater. Trans. A*, 2006, vol. 37A, pp. 1949–62.

25. T.M. Pollock, J. Dibbern, M. Tsunekane, J. Zhu, and A. Suzuki: *JOM*, 2010, vol. 62, pp. 58–63.
26. J. Valdes, P. King, and X. Liu: *Metall. Mater. Trans. A*, 2010, vol. 41A, pp. 2408–16.
27. R. Schadt, I. Wagner, J. Preuhs, and P.R. Sahm: *Superalloy 2000*, T.M. Pollock, R.D. Kissinger, and R.R. Bowman, eds., TMS, Warrendale, PA, 2000, pp. 211–18.
28. P. Auburtin: Ph.D. Dissertation, University of British Columbia, Vancouver, B.C., Canada, 1998.
29. P. Auburtin, T. Wang, S.L. Cockcroft, and A. Mitchell: *Metall. Mater. Trans. B*, 2000, vol. 31B, pp. 801–11.
30. P. Auburtin, S.L. Cockcroft, A. Mitchell, and T. Wang: *Superalloy 2000*, T.M. Pollock, R.D. Kissinger, and R.R. Bowman, eds., TMS, Warrendale, PA, pp. 255–61.
31. D. Ma and A. Bührig-Polaczek: *Int. J. Cast Metals Res.*, 2009, vol. 22, pp. 422–29.
32. D. Ma and A. Bührig-Polaczek: *Int. J. Mater. Res.*, 2009, vol. 100, pp. 1145–51.
33. L. Li: Ph.D. Dissertation, Auburn University, Auburn, AL, 2002.
34. D. Ma, M. Mathes, B. Zhou, and A. Bührig-Polaczek: *Adv. Mater. Res.*, 2011, vol. 278, pp. 114–19.
35. A.K. Sample and A. Hellawell: *Metall. Trans. A*, 1984, vol. 15A, pp. 2163–73.
36. J.R. Sarazin and A. Hellawell: *Metall. Trans. A*, 1988, vol. 19A, pp. 1861–71.
37. R.N. Grugle and L.N. Brush: *JOM*, 1997, vol. 49, pp. 26–30.
38. X. Wang, R.M. Ward, M.H. Jacobs, and M.D. Barratt: *Metall. Mater. Trans. A*, 2008, vol. 39A, pp. 2981–89.